Investigation of Crack Resistance in Single Walled Carbon Nanotube Reinforced Polymer Composites Based on FEM

H. Hemmatian[1], A. Fereidoon[1], M. Rajabpour[2]

Abstract

Carbon nanotube (CNT) is considered as a new generation of material possessing superior mechanical, thermal and electrical properties. The applications of CNT, especially in composite materials, i.e. carbon nanotube reinforced polymer have received great attention and interest in recent years. To characterize the influence of CNT on the stress intensity factor of nanocomposites, three fracture modes (opening, shearing and tearing) are considered. The stress intensity factor of nanocomposites is evaluated using a representative volume element (RVE) based on the continuum mechanics and finite element method (FEM). Inter-atomic interactions of CNT are simulated by beam elements in the finite element (FE) model. Non-linear spring-based line elements are employed to simulate the van der Waals (vdW) bonds. In all fracture modes, the stress intensity factor was determined for pure matrix and matrix reinforced with single-walled carbon nanotube (SWCNT). Numerical results indicate that the load carrying capacities of the CNTs in a matrix are evident. Addition of CNTs in a matrix can increase the stiffness of the composite. Finally, the results showed that utilizing of SWCNT decreased the stress intensity factor and improved crack resistance.

Keywords: Stress intensity factor; Fracture modes; Nanocomposite; Carbon nanotubes; Finite element model

1. Introduction

In the last few years, single-walled carbon nanotube polymer composites have generated considerable interest in the materials research community because of their potential for large increases in strength and stiffness, when compared to conventional carbon-fiber-reinforced polymer composites. Even though some nanotube composite materials have been characterized experimentally [1-3], the development of these materials can be greatly facilitated by using computational methods that allow for parametric studies of the influence of material and geometry.

Carbon nanotubes (CNTs) have been used as reinforcements in polymer–matrix composites due to their superior mechanical properties [4-6]. Carbon nanotubes, however, do not bond well to polymers [7, 8], and their interactions are due to the van der Waals force [9-12], which is much weaker than covalent bonds.

Unique atomic structure, very high aspect ratio and extra ordinary mechanical properties make CNTs ideal reinforcing materials in nanocomposites. While a significant number of the existing studies have been focused on the stiffness and strength of CNT-reinforced composites [13-16], relatively few research studies have dealt with the fracture behavior of these nanocomposites in the presence of a pre-existing crack. Recent investigations [17] have shown that CNTs when aligned perpendicular to cracks is able to slow down the crack growth by bridging up the crack faces.

Contradictory reports have been given on how different types of CNTs and different methods of material processing affect mode I fracture toughness (K_{Ic}) of nanocomposites. For instance, Gojney et al. [18] produced epoxy/double walled CNT nanocomposite by the calendaring technique and measured K_{Ic} of the resulting nanocomposite using the compact tension (CT) specimen. Fracture toughness was found to increase 18.5% and 27.7% at a CNT content of 0.1 and 1 wt.%, respectively. In the same way, Thostenson and Chou [19] used the calendaring technique to disperse multi-walled carbon nanotubes in epoxy and

1- Faculty of Mechanical Engineering, Semnan University, Semnan, Iran
2- Young Researchers Club, Semnan branch, Islamic Azad University, Semnan, Iran

Corresponding author:
H. Hemmatian. Faculty of Mechanical Engineering, Semnan University, Semnan, Iran
Email: hoseinhemmatian@gmail.com

used single-edge notch bend (SENB) specimen to measure K_{Ic}.

Arai et al. [20] have reported 50% and 150% increase in the mode I and mode II fracture toughness of the epoxy/carbon fiber laminates modified by nano-carbon fibers. Moreover, the addition of 5 wt.% of cup-stacked CNT to epoxy increased the interlaminar fracture toughness up to 300% [21]. The effect of CNT dimensions on the fracture properties of nanocomposites is another important issue which requires a careful investigation. A few researchers have investigated the effect of CNT dimensions on different properties of nanocomposites [22, 23].

Fundamental to Li et al. [24] approach, CNTs are considered as geometrical space-frame structures. Therefore, CNTs can be analyzed by classical structural mechanics. In this paper, based on the concept of Li et al. [25], three-dimensional (3D) FE models are proposed for three fracture modes. In all fracture modes the stress intensity factor was determined for pure matrix and matrix reinforced with SWCNT.

2. FE modeling

2.1. Nanotube

CNTs atoms are bonded together with covalent bonds forming a hexagonal lattice. The displacement of individual atoms under an external force is constrained by the bonds. Therefore, the total deformation of the nanotube is the result of the interactions between the bonds. By considering the bonds as connecting load-carrying elements, and the atoms as joints of the connecting elements, CNTs may be simulated as space-frame structures. The 3D FE model is developed using the ANSYS commercial FE code. For the modeling of the bonds, the 3D elastic BEAM4 element is used. The properties of these elements are obtained by linking the potential energy of bonds (from a chemical point of view) and the strain energy of mechanical elements (from a mechanical point of view). To represent the covalent bond between carbon atoms, a circular beam of length l, diameter d, Young's modulus E, and shear modulus G was considered [25]. The required properties of the beam element are given in Table 1.

Table 1. The properties of beam elements for real carbon nanotube [25].

Nanotube diameter, d	1.466 Å
Cross-sectional area, A	1.68794 $Å^2$
The length of carbon–carbon bond	1.421 Å
Polar inertia momentum, I_{xx}	0.453456 $Å^4$
Inertia momentum, $I_{zz} = I_{yy} = I$	0.22682 $Å^4$
Young's modulus, E	5.488 $\frac{N}{Å^2}$
Shear modulus, G	8.711 $\frac{N}{Å^2}$

The thickness of CNT is selected as 0.34 nm and center of the carbon atoms in the CNT are placed at the midsection of the tube thickness. The FE meshes of CNT are shown in Fig. 1.

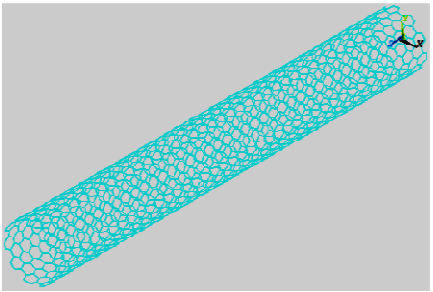

Fig. 1. Isometric view of the FE meshes of the (10, 10) carbon nanotube.

2.2. Inter-phase between nanotube and polymer

The bonding between embedded CNT and its surrounding polymer takes place through vdW and electrostatic interactions in the absence of chemical functionalization. Electrostatic interactions can be neglected in comparison with vdW interactions, since vdW contributes more significantly in three higher orders of magnitude than electrostatic energy [26]. Therefore, the bonding via vdW interactions is considered here. The vdW forces are most often modeled using famous Lennard-Jones [27].

$$F_{vdw} = 4\frac{\varepsilon}{r}\left[-12\left(\frac{\sigma}{r}\right)^{12} + 6\left(\frac{\sigma}{r}\right)^{6}\right] \quad (1)$$

where r is the separation distance between the pair of atoms, $\sqrt[6]{2}\,\sigma$ is the equilibrium distance between atoms, ε is the bond energy at the equilibrium distance, and σ is the vdW

separation distance. For the vdW interaction between a carbon atom and a –CH2– unit of epoxy, $\varepsilon = 0.004656\ ev$ and $\sigma = 0.3825\ nm$ [28].

$$x = r - \sqrt[6]{2}\sigma \quad (2)$$

$$F(x) = -24\frac{\varepsilon}{\sigma}\left[2\left(\frac{\sigma}{x+\sqrt[6]{2}\sigma}\right)^{13} - \left(\frac{\sigma}{x+\sqrt[6]{2}\sigma}\right)^{7}\right] \quad (3)$$

where x is the distance from the equilibrium distance for the vdW force between carbon atoms. This relation is illustrated in Fig. 2.

The vdW interactions between carbon atoms of CNT and the nodes of inner surface of surrounding resin is modeled using three-dimensional (3D) non-linear spring and the corresponding data of force-displacement curve [27]. COMBIN39 element is used for this purpose and the parameters are adjusted to obtain translational spring. A macro is written to create elements between those nodes which their distance is lower than 0.85 nm. For sake of simplicity, the spring elements are only created between carbon atoms of the CNT and the inner surface of the resin.

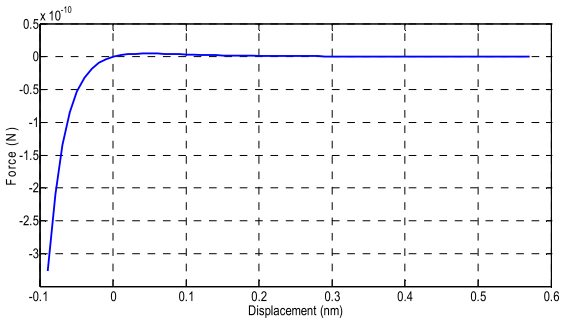

Fig. 2. Variation of vdW force against displacement.

2.3. Matrix

For matrix modeling, SOLID45 elements were utilized. This element is used for the 3-D modeling of solid structures. The element is defined by eight nodes having three degrees of freedom at each node: translations in the nodal x, y, and z directions. Epoxy by Young modulus of 3.972 GPa is considered as matrix [29]. In this paper assumed that nanocomposite consist of %5 Volume fraction of CNT. The FE meshes of RVE that used for crack analysis are shown in Fig. 3. The elements of crack tip are refined to increase the accuracy of analysis.

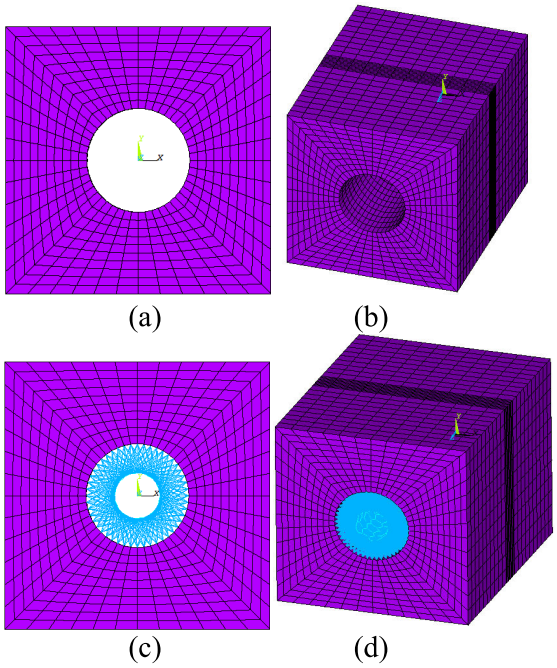

Fig. 3. The FE meshes for crack analysis: (a), (b), matrix, (c), (d), RVE

3. Stress intensity factor

In fracture mechanics based on crack surfaces displacement, three crack modes as flowing are considered (as shown Fig. 4) [30]:

Opening mode (tensile mode), I: The two crack surfaces are pulled apart in the y direction, but the deformations are symmetric about the x–z and x–y planes.

Shearing mode (sliding mode), II: The two crack surfaces slide over each other in the x-direction, but the deformations are symmetric about the x–y plane and skew-symmetric about the x–z plane.

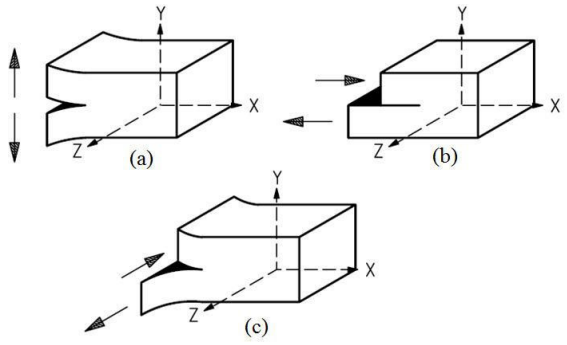

Fig. 4. Independent modes of crack displacements: (a) Opening mode, (b) Shearing mode, (c) Tearing mode.

Tearing mode (out-of-plane), III: The crack surfaces slide over each other in the z-direction, but the deformations are skew-symmetric about the x−y and x−z planes.
The computation of stress intensity factors in the finite element analysis is performed using the J integral technique with ANSYS Parametric Design Language (APDL). In this paper for similar loading, comparison of stress intensity factors between neat matrix and nanocomposite are performed.

4. Results and discussion

In this study, fracture analysis of nanocomposite reinforced with three different CNT with chirality (5, 5), (10, 10), (20, 20), are implemented. In Fig. 5, normalized stress intensity factors (ratio of nanocomposite stress intensity factor to that of neat matrix) in fracture modes have been plotted against chirality. Stress and displacement contours of neat matrix and nanocomposite that reinforced with nanotube (5, 5) are shown in Figs. 6, 7, 8. Results indicate that with the addition of CNT to matrix, stress intensity factors decreased. Also, by increasing the chirality, crack resistance enhances. Figs. 6, 7 and 8 indicate that in all modes, maximum stress occurred in contact location of CNT and crack. Carbon nanotube resists against crack propagation and bridges on the crack path. This behavior of CNT is known as bridging phenomenon. On the other hand bridging arises in all three modes and stress intensity factor decreases. This phenomenon is reported in experimental research too [31-36]. Therefore, adding CNT to matrix improves the crack resistance which is considerable in opening and tearing modes.

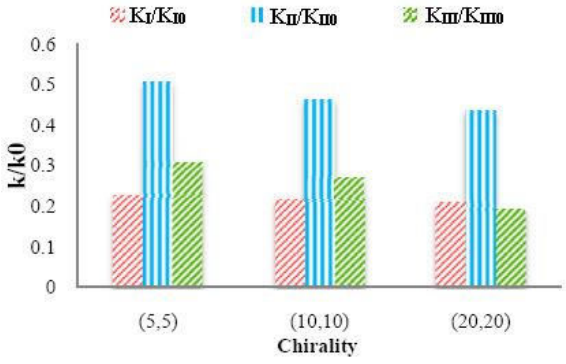

Fig. 5. Normalized stress intensity factors against chirality.

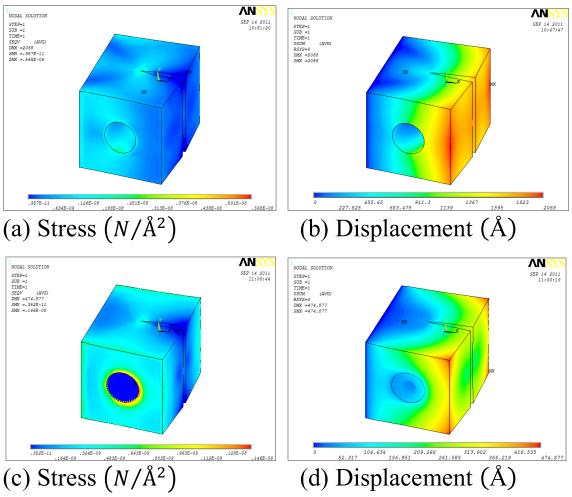

Fig. 6. Stress and displacement contours of opening mode: (a), (b) neat matrix, (c), (d) nanocomposite.

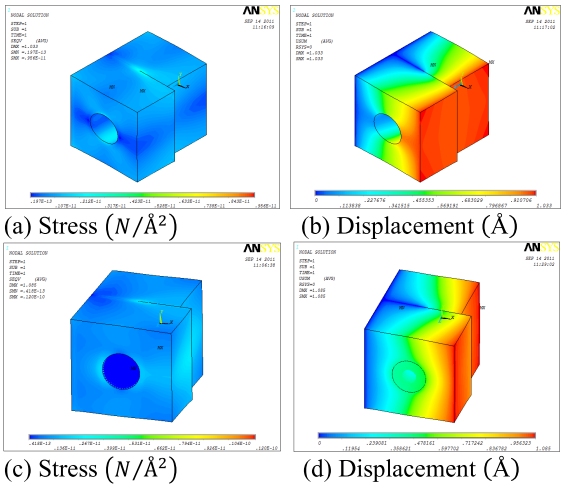

Fig. 7. Stress and displacement contours of shearing mode: (a), (b) neat matrix, (c), (d) nanocomposite.

In modeling, chirality, length, weight percentage and diameter of CNT have importance. But in experimental method only weight percentage is considered. Hence appropriate verification between experimental and modeling results is very difficult. Moreover the experimental results are very different, but in all works by adding CNT to matrix, fracture behaviors are improved [37-41].

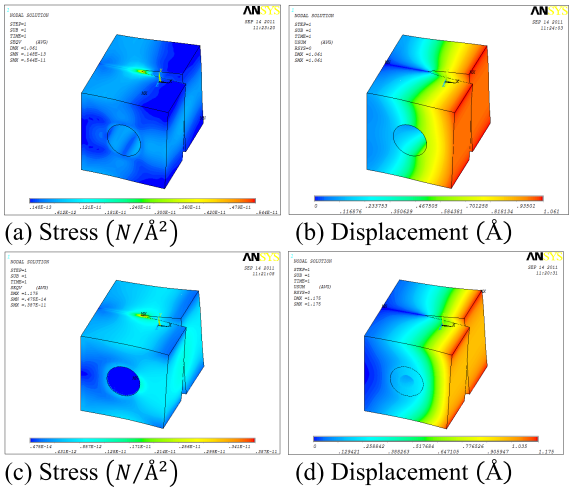

(a) Stress $(N/Å^2)$ (b) Displacement (Å)

(c) Stress $(N/Å^2)$ (d) Displacement (Å)

Fig. 8. Stress and displacement contours of tearing mode: (a), (b) neat matrix, (c), (d) nanocomposite.

5. Conclusions

A 3D study of fracture modes for epoxy/CNT has been performed using FEM. Stress intensity factor is computed for three fracture modes. Influence of CNT on the stress intensity factor of nanocomposites and propagating crack is studied. To create the FE models, nodes are placed at the locations of carbon atoms and the bonds between them are modeled using three-dimensional elastic beam elements. Van der Waals bonds are simulated by employing the non-linear spring elements. As the FE model comprises small number of elements, it performs under minimal computational time by requiring minimal computational power. The results of the study indicate that CNTs have a significant influence on preventing crack propagation. Results represent that by adding CNT, stress intensity factors decreased and consequently crack resistance increased. Also, by increasing the chirality, crack resistance improved. Finally, by adding CNT to matrix, fracture properties improvement of matrix is evident.

References

1. Ajayan, P. M., Schadler, L. S., Giannaris, S. C., Rubio, A., *Adv. Mater*., Vol. 12 (2000) pp. 750-53.
2. Gong, X., Liu, J., Baskaran, S., Voise, R. D., Young, J. S., Chem. *Mater*., Vol. 12 (2000) pp. 1049-52.
3. Qian, D., Dickey, E. C., Andrews, R., Rantell, T., *Appl. Phys. Lett*., Vol. 76 (2000) pp. 2868-70.
4. Thostenson, E. T., Li, C. Y., Chou, T. W., *Compos. Sci. Technol*., Vol. 65 (2005) pp. 491-516.
5. Maruyama, B., Alam, H., *SAMPE J*., Vol. 38 (2002) 59.
6. Breuer, O., Sundararaj, U., *Polym. Compos*., Vol. 25 (2004) pp. 630-45.
7. Schadler, L. S., Giannaris, S. C., Ajayan, P. M., *Appl. Phys. Lett*., Vol. 73 (1998) pp. 3842-44.
8. Lau, K. T., Shi, S. Q., *Carbon,* Vol. 40 (2002) 2965.
9. Frankland, S. J. V., Caglar, A., Brenner, D. W., Griebel, M., *J. Phys. Chem*., B, Vol. 106 (2002) pp. 3046-48.
10. Li, C. Y., Chou, T. W., *J. Nanosci. Nanotechnol*., Vol. 3 (2003) 423.
11. Wong, M., Paramsothy, M., Xu, X. J., Ren, Y., Li, S., Liao, K., *Polymer,* Vol. 44 (2003) pp. 7757-64.
12. Gou J., Minaie, B., Wang, B., Liang, Z., Zhang, C., *Comput. Mater*. Sci., Vol. 31 (2004) pp. 225-36.
13. Montazeri, J. Javadpour, A. Khavandi, A. Tcharkhtchi, A. Mohajeri, *Mater. Des.,* Vol. 31 (2010) pp. 4202-08.
14. Bal, S., *Mater. Des.,* Vol. 31 (2010) pp. 2406-13.
15. Montazeri, A. Khavandi, J. Javadpour, A. Tcharkhtchi, *Mater. Des.*, Vol. 31 (2010) pp. 3383-88.
16. Bogdanovich, E., Bradford, P. D., *Composites Part A,* Vol. 41 (2010) pp. 230-37.
17. Lau, K. T., Hui, D., *Carbon,* Vol. 40 (2002) pp. 1605-06.
18. Gojny, F. H, Wichmann, M. H. G., Kopke, U., Fiedler, B., Schulte, K., *Compos. Sci. Technol*., Vol. 64 (2004) pp. 2363-71.
19. Thostenson, E. T., Chou, T. W., *Carbon,* Vol. 44 (2006) pp. 3022-29.
20. Arai M., Noro Y., Sugimoto, K. i., Endo, M., *Compos. Sci. Technol*., Vol. 68 (2008) pp. 516-25.
21. Yokozeki, T., Iwahori, Y., Ishibashi, M., Yanagisawa, T., Imai, K., Arai, M., *Compos. Sci. Technol.,* Vol. 69 (2009) pp. 2268-73.
22. Wu, D., Wu, L., Zhou, W., Y. Sun, M. Zhang, *J. Polym. Sci., Part B: Polym. Phys*., Vol. 48 (2010) pp. 479-89.
23. Hernández-Pérez, A., Avilés, F., May-Pat, A., Valadez-González, A., Herrera-Franco, P. J.,

Bartolo-Pérez, P., *Compos. Sci. Technol.,* Vol. 68 (2008) pp. 1422-33.
24. Li T., Chou, W., *Compos. Sci. Technol.,* Vol. 63 (2003) pp. 1517-24.
25. Li, T., Chou, W., *Int. J. Solid. Struc*. Vol. 40 (2003) pp. 2487-99.
26. Gou, J., Minaei, B., Wang, B., Liang, Z., Zhang, C., *Comput. Mater. Sci*., Vol. 31 (2004) pp. 225-36.
27. L. Battezzatti, C. Pisani, F. Ricca, *J. Chem. Soc*. *Faraday Trans. 2*, Vol. 71 (1975) pp. 1629-39.
28. Frankland, S. J. V., Harik, V. M., Odegard, G. M., Brenner, D. W., Gates, T. S., *Compos. Sci. Technol*., Vol. 63 (2003) pp. 1655-61.
29. Kaw K., *Mechanics of composite materials*, CRC Press; Taylor & Francis Group, Ch. 1 (2006) 28.
30. Saouma, V. E., *Fracture mechanics*, Boulder, Ch. 6 (2000) 11.
31. Gojny, F. H., Wichmann, M. H. G., Fiedler, B., Schulte, K., *Compos. Sci. Technol*., Vol. 65 (2005) pp. 2300-13.
32. Mirjalili, V., Hubert, P., *Compos. Sci. Technol*., Vol. 70 (2010) pp. 1537-43.
33. Chan, K. S., Lee, Y. D., Nicolella, D. P., Furman, B. R., Wellinghoff, S., Rawls, R., *ENG. FRACT. MECH.,* Vol. 74 (2007) pp. 1857-71.
34. Zeng, Q. H., Yu, A. B., Lu, G. Q., *Prog. Polym. Sci*., Vol. 33 (2008) pp. 191-269.
35. Gonza´lez, C., LLorca, J*., Acta Mater.,* Vol. 54 (2006) pp. 4171-81.
36. D. Wu, S. Meure, D. Solomon, *Prog. Polym. Sci*., Vol. 33 (2008) pp. 479-522.
37. Lachman, N., Wagner, H. D., *Composites: Part A,* Vol. 41 (2010) pp. 1093-98.
38. Rafiee, R., Fereidoon, A., Heidarhaei, M., *Comput. Mater*. Sci., Vol. 56 (2012) pp. 25-28.
39. Davis, D. C., Whelan, B. D., *Composites: Part B,* Vol. 42 (2011) pp. 105-16.
40. M. R. Ayatollahi, S. Shadlou, M. M. Shokrieh, *Mater. Des.,* Vol. 32 (2011) pp. 2115-24.
41. Zhou, Y., Jeelani, M. I., Jeelani, S., *Mater. Sci. Eng., A ,* Vol. 506 (2009) pp. 39-44.